Fission Product Yield Modeling and Evaluation

A. E. Lovell[1]*, *T.* Kawano[1], *P.* Talou[1,2], and *G.* Rusev[1]

[1]Los Alamos National Laboratory, Los Alamos, NM 87545, USA
[2]Stardust Science Labs, Santa Fe, NM 87507, USA

Abstract. Although independent and cumulative fission product yields have been a part of evaluated libraries for decades, there have been few updates over the years. The fission product yield sub-library in the ENDF/B-VIII.0 library is still largely based on the evaluation of England and Rider from the mid-90's, with only more recent updates to the energy dependence of ^{239}Pu below 2 MeV and fixes to isomeric states and missing fission products. Over the past several years, there have been a wealth of new measurements of independent and cumulative fission product yields, particularly those with short half-lives, and there have been significant improvements in the modeling of prompt and delayed fission observables. Here, we describe recent progress in the improvement of fission product yield calculations, using the `BeoH` code and the underlying Hauser Feshbach Fission Fragment Decay (HF^{3}D) model, developed at Los Alamos National Laboratory. We will describe our recent calculations for consistent prompt and delayed fission observables for major and minor actinides, including new work investigating isomeric ratios. We will detail the ongoing evaluation process for energy-dependent fission product yields from thermal up to 20 MeV incident neutron energy and some validation work that has been performed for these new fission product yield calculations. Additionally, we will discuss future perspectives of this work, highlighting the need for additional data.

1 Introduction

Fission product yields (FPYs) have recently received a significant amount of attention by the nuclear data and basic science communities. Many new measurements have recently been performed [1–5] investigating both neutron-induced and photon-induced FPYs. A recent Workshop for Applied Nuclear Data Activities (WANDA) meeting had one full-day session dedicated to the past and future of FPYs [6]. An international effort has been coordinated by the International Atomic Energy Agency (IAEA) on the subject of FPYs [7], to bring together evaluators across the globe. Additionally, many modeling improvements have been made in recent years that aim to consistently calculate FPYs, prompt, and delayed fission observables, including the construction of covariances, e.g. [8–13].

For the ENDF/B libraries, the independent and cumulative FPY evaluations are still largely based on the evaluation of England and Rider [14] from the mid-1990s. Since then, there have been only minor updates. For the ENDF/B-VII.1 evaluation, a point at 2 MeV incident neutron energy was included for the FPYs of ^{239}Pu [15] to better describe their energy dependence in the few MeV region and to resolve a long-standing disagreement between Los Alamos and Livermore National Laboratories [15, 16]. Additionally, for the ENDF/B-VIII.1 release, there were several minor corrections [17–19]. One was a correction to the uncertainties of 17 cumulative FPYs near stability that were anomalously large. Four independent FPYs were modified to take into account that isomers for ^{109}Ru and ^{109}Rh have not been experimentally confirmed. Finally, there were corrections to the thermal neutron-induced FPYs of ^{241}Pu that have shown a discontinuity since ENDF/B-VI.2. Unlike much of the rest of the ENDF/B library, there has been no previous push to include full covariances with the evaluation, only standard deviations are given. In fact, a format does not currently exist to include these covariances.

In this work, we discuss recent updates to FPY modeling and evaluation efforts. In Sec. 2, we overview the `BeoH` code and underlying Hauser-Feshbach Fission Fragment Decay (HF^{3}D) model along with the Kalman filter routine used for evaluation work. We show selected results for major actinides from this procedure in Sec. 3, along with overview of other calculations that can be done in the same framework, including minor actinide evaluations and calculations of *R*-values, isomeric ratios, and photofission. Finally, we conclude in Sec. 4.

2 Theory

2.1 Fission product yield modeling

`BeoH` is a deterministic, fission decay code that uses the Hauser-Feshbach Fission Fragment Decay (HF^{3}D) model to calculate prompt and delayed fission observables [8, 9]. Information about the compound nucleus before and after scission is required. The pre-scission information is calculated from `CoH`$_3$ [20] and includes inputs such as the

*e-mail: lovell@lanl.gov

most probable excitation energy causing fission, the multi-chance fission probabilities, and energies of pre-fission neutrons. After scission, information about the fission fragment initial conditions is necessary input. To calculate the pre-neutron emission distributions, $Y(A, Z, \mathrm{TKE}, J, \pi)$, first every possible fission fragment pair, (A_L, Z_L) and (A_H, Z_H), is generated and their relative probabilities are constructed from joint $Y(A, Z)$ distributions. The pre-neutron emission mass distribution, $Y(A)$, is taken to be a sum of three Gaussians whose weights, means, and standard deviations are fitted to available experimental data and dependent on the incident neutron energy. The charge distribution is given by the Wahl systematics [21].

The total kinetic energy, TKE, of the two fission fragments is linear as a function of incident neutron energy. It is split between the two fission fragments based on kinematics. The Q-value of the fission fragment split determines the total excitation energy, TXE, of the pair, which is then shared between the two fragments based on a ratio of temperatures. Once the excitation energy of each fragment is determined, its population can be constructed as a function of the excitation energy, spin, and parity. Once these initial conditions of the fission fragments are set, Hauser-Feshbach statistical theory [22] is used to de-excite the fragments via emission of prompt neutrons and γ rays. For details, see [9].

Prompt observables, such as the average neutron multiplicity, are calculated as a weighted sum of the results of the Hauser-Feshbach calculations from each fission fragment. In these sums the probability for pre-fission neutron emission is taken into account. Because we consider incident neutron energies from thermal to 20 MeV, we generally have to consider first, second, third, and fourth chance fission.

`BeoH` additionally calculates delayed observables, such as the average delayed neutron multiplicity and the cumulative fission product yields. At this point in the calculation, we keep track of the metastable states of the isotopes that are produced after the Hauser-Feshbach decay, and the cumulative FPYs, $Y_C(A, Z, M)$, are calculated from the independent FPYs, $Y_I(A, Z, M)$, by following all possible decays of the independent FPYs and adding them to the initial ones. This procedure can be written as follows:

$$\begin{aligned} Y_C(A_i, Z_i, M_i) &= Y_I(A_i, Z_i, M_i) \\ &+ \sum_j^N \sum_l^{L_j} Y_C(A_j, Z_j, M_j) b_{jl} \delta_{jl,i}, \end{aligned} \quad (1)$$

where $b_{j\ell}$ are the branching ratios with L_j total decay modes, N is the total number of nuclei that produce the i^{th} nucleus, and $\delta_{j\ell,i}$ connects $Y_C(A_j, Z_j, M_j)$ with $Y_C(A_i, Z_i, M_i)$. Currently, the decay data are taken from the ENDF/B-VIII.0 library [23], but we are working with collaborators at Brookhaven National Laboratory to take into account updates to decay data that are being made for future ENDF/B releases. In this way, the new FPY evaluation will be consistent with the decay data available in the same library.

2.2 Evaluation methodology

To perform the parameter optimization and evaluation, we use a Kalman filter routine [24]. This version of the Kalman filter makes a linear approximation between the model parameters, $\mathbf{x}$, and outputs, $f(\mathbf{x})$, such that

$$f(\mathbf{x}_1) = f(\mathbf{x}_0) + \mathbb{C}\delta\mathbf{x}. \quad (2)$$

Changes in the model values, $\delta\mathbf{f} = f(\mathbf{x}_1) - f(\mathbf{x}_0)$, are linearly related to changes in the model parameters, $\delta\mathbf{x} = \mathbf{x}_1 - \mathbf{x}_0$, through a sensitivity matrix

$$\mathbb{C}_{ij} = \left.\frac{\partial f(\mathbf{x})}{\partial x_j}\right|_{\mathbf{x}=\mathbf{x}_0}. \quad (3)$$

The index i runs over all incident energies for the observables included in the evaluation (here, cumulative fission product yields along with prompt and delayed neutron multiplicities).

In Eq. (2), the parameter changes are determined through matrix algebra by

$$\delta\mathbf{x} = \mathbb{P}\mathbb{C}^T\mathbb{V}^{-1}(\phi - f(\mathbf{x}_0)), \quad (4)$$

where $\mathbb{P}$ is the posterior parameter covariance, $\mathbb{V}$ is the covariance of the experimental data, and ϕ is the vector of experimental mean values. Here, we assume that $\mathbb{V}$ is diagonal, with the squared experimental uncertainties on the diagonal, but recent efforts to create templates of experimental uncertainties [25] would allow us to include realistic off-diagonal elements, even with limited information reported on the sources and magnitudes of the experimental systematic uncertainties. The posterior parameter covariance matrix is also calculated through linear algebra,

$$\mathbb{P} = (\mathbb{X}^{-1} + \mathbb{C}^T\mathbb{V}^{-1}\mathbb{C})^{-1}. \quad (5)$$

Here, we additionally require a prior parameter covariance matrix, which we assume only contains the parameter uncertainties on the diagonal, which are taken to be 5% of the baseline values. The model values can be updated through Eq. (2) or by running the updated parameter values, $\mathbf{x}_1$, back through the model. We take the second approach, as we perform several iterations of Eqs. (4) and (5) where we include subsequently more FPY data into the optimization and evaluation with each iteration of the Kalman filter, instead of attempting to optimize all of the data at once. We begin our optimization by including the fission fragments with the largest cumulative yield and successively include those fragments with smaller cumulative yields. We include in our optimization parameters for $Y(A)$, Wahl scaling factors (see [8, 9]), TKE, and the spin cutoff parameter.

Covariances across observables can be calculated through

$$\mathbb{F} = \mathbb{C}\mathbb{P}\mathbb{C}^T, \quad (6)$$

with $\mathbb{C}$ and $\mathbb{P}$ defined as in Eqs. (3) and (5). The current ENDF/B-VIII.0 evaluation [23] and other global evaluations do not currently contain full covariances between either FPY values or incident neutron energies, although a current Coordinated Research Project (CRP) at the IAEA is coordinating the international community on this effort [7].

3 Results

3.1 Major actinide evaluations

Using a combination of the Kalman filter and available, curated experimental data (where many outliers were removed from the fitting procedure), we calculated independent and cumulative fission product yields for ^{239}Pu, ^{235}U, and ^{238}U from thermal to 20 MeV incident neutron energies. In the top panel of Fig. 1, we show an example of the cumulative fission product yields calculated this way, for ^{95}Zr (solid lines and associated shaded bands), which is compared to some available experimental data (open squares), and the ENDF/B-VIII.0 evaluation (filled stars). We first note that there is more significant coverage of experimental data across incident neutron energies for ^{238}U compared to ^{235}U and ^{239}Pu, particularly between the opening of second-chance fission (~5 MeV) and 14 MeV, although newly measured data, e.g. [1, 5], is beginning to fill in these energy regions for the other major actinides. We also see that the availability of more recently measured experimental data, as for ^{239}Pu between 2 and 5 MeV, provides the justification for an incident energy dependence in our optimized calculations that is not currently included in the ENDF/B-VIII.0 evaluation.

In the lower panel of Fig. 1, we show the relative uncertainty resulting from this optimization compared to the uncertainty on the experimental data and ENDF/B-VIII.0 evaluation. We see that the calculated uncertainties are, for the most part, smaller than the experimental uncertainties. This feature is common within the framework of the Kalman filter and often requires that the evaluated uncertainties be rescaled upwards. We note here that these uncertainties are still preliminary as we determine whether they are realistic or some factor needs to be introduced to take into account unrecognized systematic uncertainties and/or stiffness in the model.

However, one of the major updates to the FPY evaluation that is being made within this methodology is the inclusion of full covariances between FPY values, instead of only including the uncertainties (diagonal values). Within the Kalman filter framework described in Sec. 2.2, we are able to produce covariances simultaneously with the evaluated parameters and mean values. There is significant structure seen in the correlations between the FPYs for a given incident neutron energy, and this structure changes as a function of incident neutron energy. This structure comes mainly from correlations between isotopes of the same element and mass chains. For more details, see [26].

Additionally, within the same HF^{3}D framework, we can calculate the independent and cumulative FPYs for minor actinides. Typically, there are significantly fewer experimental measurements for cumulative FPYs for the minor actinides, and the data are focused largely around the thermal energy point. Here, we can leverage the fact that many compound nuclei fission at higher incident neutron energies due to the inclusion of multi-chance fission within the model, and use these optimized parametrizations in `BeoH` as a prior for the minor actinide calculations. Therefore, even if there are few data, we can put a higher confidence in these calculations. Currently, we have preliminary results for many minor U and Pu isotopes.

3.2 *R*-value validation

To validate our FPY calculations, we compute the *R*-values for many isotopes. The *R*-value is defined as a ratio of ratios, for example that of ^{147}Nd for ^{239}Pu,:

$$R_{147} = \frac{Y_{147}(\mathrm{Pu})}{Y_{99}(\mathrm{Pu})} \frac{Y_{99}(\mathrm{U_{th}})}{Y_{147}(\mathrm{U_{th}})}, \tag{7}$$

where Y_{147}(Pu) and Y_{99}(Pu) are the cumulative FPYs for ^{147}Nd and ^{99}Mo for ^{239}Pu at a given incident energy, and $Y_{147}(\mathrm{U_{th}})$ and $Y_{99}(\mathrm{U_{th}})$ are the cumulative FPY for thermal neutron-induced fission of ^{235}U producing ^{147}Nd and ^{99}Mo. Historically, these *R*-values were measured by irradiating ^{239}Pu samples in critical assemblies. The samples were placed at different distances from the center of the critical assembly, which changes the neutron flux and thus the effective neutron energy of the reaction. Currently, we can model the full assembly and calculate the flux as a function of location in the assembly and incident neutron energy using MCNP. These fluxes are then folded with the incident energy dependent *R*-values calculated using FPYs from `BeoH` to be compared with the experimental data. When plotting the results as a function of location from the center of the critical assembly, the calculated *R*-values are consistent with the experimental ones within error bars. However, as we currently do not include the correlations between calculated FPYs at each incident neutron energy, we expect that the uncertainties on the calculated *R*-values will reduce.

3.3 Isomeric ratios

We have additionally begun to investigate the energy-dependent isomeric ratios of the fission product yields for these major actinides. In the ENDF/B-VIII.0 (and earlier evaluations), the isomeric states are calculated using the Madland-England approach [27], which is a one-parameter model for calculating the splitting of the strength between the ground state and isomeric state of fission fragments. As can be seen from Fig. 2, the newly recompiled recommended value for the isomeric ratio of ^{98}Y from [28] (open triangle) is significantly closer to the `BeoH` values (filled circles) than the current ENDF/B-VIII.0 evaluated values (open stars). Although we show an example only for ^{98}Y, other comparisons also indicate that the Madland-England approach is too simplified. Further investigations are underway for many more isomeric ratios, including comparisons with preliminary, newly measured experimental data [29]. These studies give us insight into the nuclear structure of the relevant isotopes and can point to needed future measurements of this structure.

3.4 Photofission

The HF^{3}D framework has also been recently extended to include modeling of photofission [30] by taking into account the correct spin and parity dependence of the resulting compound nucleus. By using the same compound

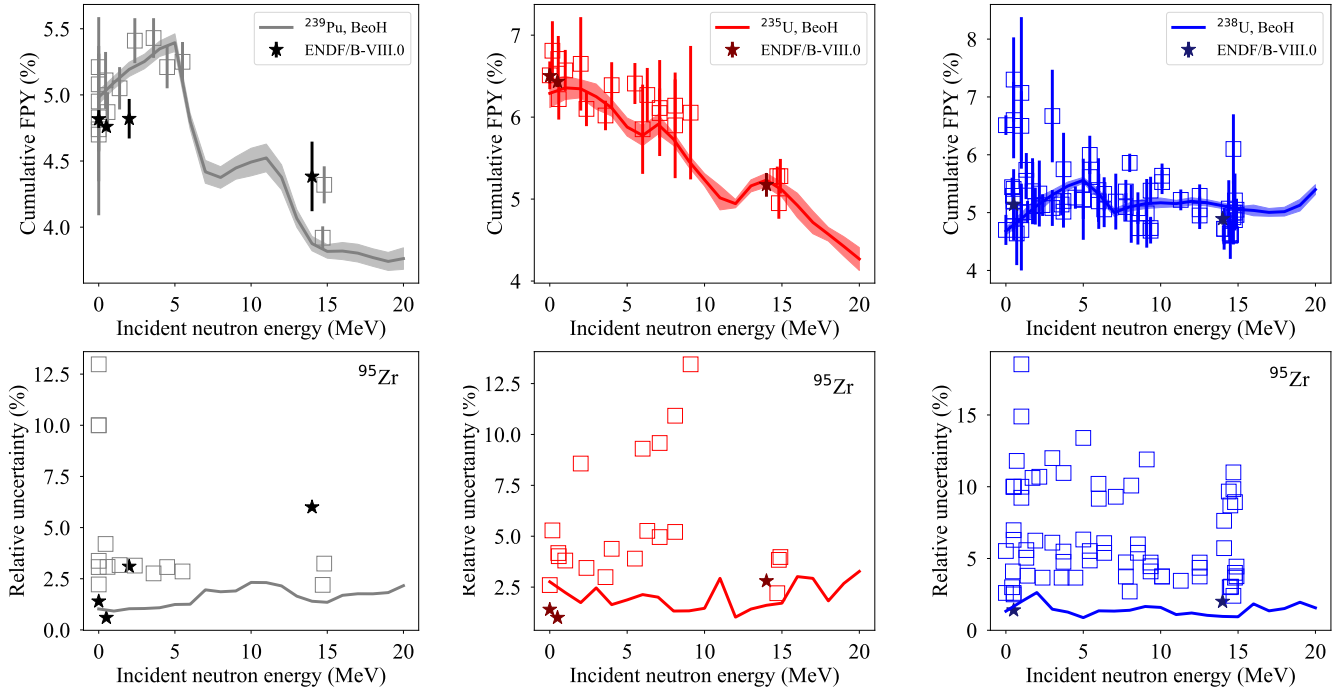

Figure 1. (Top) Cumulative fission product yields in percent for ^{95}Zr from the neutron-induced fission of ^{239}Pu (left, shades of grey), ^{235}U (middle, shades of red), and ^{238}U (right, shades of blue). (Bottom) Relative uncertainties in percent of the cumulative fission product yields for ^{95}Zr. In each panel, the BeoH calculation is given by the solid line, experimental data by the open squares, and the ENDF/B-VIII.0 evaluation by the filled stars.

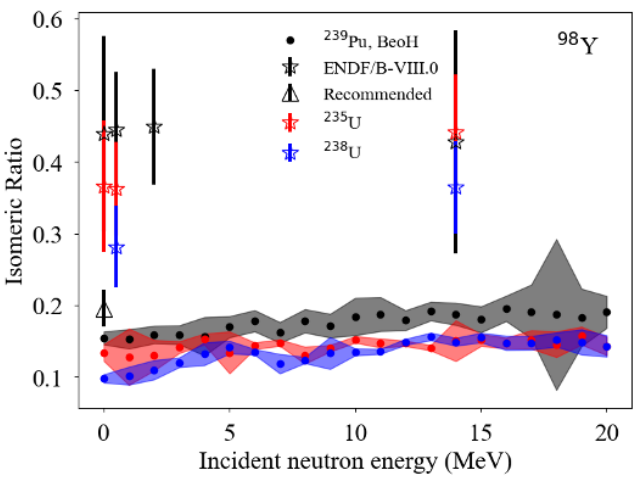

Figure 2. Isomeric ratios of ^{98}Y for the major actinides, BeoH calculations (filled circles with associated shaded bands), recommended values from [28] (open triangles), and values from ENDF/B-VIII.0 (open stars). The isomeric ratio for ^{235}U, ^{238}U, and ^{239}Pu are shown in red, blue, and black, respectively.

nucleus parameters as in [10], we are able to reproduce prompt fission observables from the photofission reaction, including prompt and delayed neutron multiplicities and cumulative mass distributions for major actinides. The only adjustment to the fission fragment initial conditions that had to be performed was for the total kinetic energy of the compound nucleus. Studying both neutron-induced and photon-induced fission reactions simultaneously could improve our knowledge of the fission fragment initial conditions, especially as the multi-chance fission channels open.

4 Conclusions

Here, we have presented modeling and evaluation results for fission product yields (FPYs) for major actinides, based on recently measured experimental data and updated theoretical models. We have used the BeoH code, with the underlying Hauser-Feshbach Fission Fragment Decay (HF^{3}D) model, developed at Los Alamos National Laboratory, to consistently calculate both prompt and delayed fission observables. Using BeoH, we simultaneously optimize the model input parameters to data for average prompt and delayed neutron multiplicities and cumulative FPYs. Recently measured experimental data leads to changes in the energy dependence of the cumulative FPYs that have not been included in previous evaluations or modeling.

We have begun to validate these new cumulative FPY calculations and evaluations using *R*-values from critical assemblies. Preliminary results show that the values for R_{147} are consistent with previous measurements within uncertainties. Future work will include repeating these *R*-value calculations with cross-isotope and cross-energy correlations to produce more realistic evaluated uncertainties.

Additionally, within the same HF^{3}D framework, we have started investigating isomeric ratios of the FPYs, performed calculations for minor actinides, and extended the model to calculate photofission reactions. The isomeric ratios have been compared to previously evaluated values and recent recommended values compiled by collaborators at Brookhaven National Laboratory. The present work indicates that the Madland-England approach of the isomeric states in the ENDF/B libraries is oversimplified. Taken together, this framework and resulting calculations provide consistent modeling of a variety of fission product yields and other fission observables from both neutron- and photon-induced fission.

This work was performed under the auspices of the U.S. Department of Energy by Los Alamos National Laboratory under Contract 89233218CNA000001 and was supported by the Office of Defense Nuclear Nonproliferation Research & Development (DNN R&D), with partial support from the Nuclear Criticality Safety Program, both funded and managed by the National Nuclear Security Administration for the U.S. Department of Energy.

References

[1] M. Gooden, et al., Nuclear Data Sheets **131**, 319 (2016). 10.1016/j.nds.2015.12.006
[2] Krishichayan, et al., Phys. Rev. C **100**, 014608 (2019). 10.1103/PhysRevC.100.014608
[3] J. Silano, et al., EPJ Web Conf. **239**, 03004 (2020). 10.1051/epjconf/202023903004
[4] A.P.D. Ramirez, et al., Phys. Rev. C **107**, 054608 (2023). 10.1103/PhysRevC.107.054608
[5] M.E. Gooden, et al., Phys. Rev. C **109**, 044604 (2024). 10.1103/PhysRevC.109.044604
[6] A.E. Lovell, et al., Tech. Rep. LA-UR-24-28785, Los Alamos National Laboratory (2024)
[7] R. Vogt, et al., Updating Fission Yield Data for Applications. (2024), Summary Report of the Second Research Coordination Meeting, 19-23 Dec 2022, Vienna, Austria, https://doi.org/10.61092/iaea.5n4h-gsyc
[8] S. Okumura, et al., J. Nucl. Sci. Tech. **55**, 1009 (2018). 10.1080/00223131.2018.1467288
[9] A.E. Lovell, et al., Phys. Rev. C **103**, 014615 (2021). 10.1103/PhysRevC.103.014615
[10] S. Okumura, et al., J. Nucl. Sci. Tech. **59**, 96 (2022). 10.1080/00223131.2021.1954103
[11] G. Kessedjian, et al., EPJ Web Conf. **281**, 00022 (2023). 10.1051/epjconf/202328100022
[12] Z. Lu, et al., EPJ Web Conf. **281**, 00015 (2023). 10.1051/epjconf/202328100015
[13] K. Fujio, et al. (2023), 2309.12653, https://arxiv.org/abs/2309.12653
[14] T.R. England, B.F. Rider, Evaluation and compilation of fission product yields 1993 (1994), LA-UR-94-3106
[15] M. Chadwick, et al., Nuclear Data Sheets **111**, 2923 (2010), Nuclear Reaction Data. 10.1016/j.nds.2010.11.003
[16] I.J. Thompson, et al., Nuclear Science and Engineering **171**, 85 (2012). 10.13182/NSE10-101
[17] A. Mattera, A. Sonzogni, Tech. Rep. BNL-220804-2021-INRE, Brookhaven National Laboratory (BNL), Upton, NY (United States) (2021), https://www.osti.gov/biblio/1762758
[18] A. Mattera, Tech. Rep. BNL-225087-2023-INRE, Brookhaven National Laboratory (BNL), Upton, NY (United States) (2023)
[19] G.P.A. Nobre, et al., ENDF/B-VIII.1: Updated nuclear reaction data library for science and applications, Nuclear Data Sheets (in prep.).
[20] T. Kawano, arXiv:1901.05641v1 (2019).
[21] A.C. Wahl, Tech. rep., Los Alamos Nat. Lab. LA-13928 (2002)
[22] W. Hauser, H. Feshbach, Phys. Rev. **87**, 366 (1952). 10.1103/PhysRev.87.366
[23] D. Brown, et al., Nuclear Data Sheets **148**, 1 (2018), Special Issue on Nuclear Reaction Data. https://doi.org/10.1016/j.nds.2018.02.001
[24] R.E. Kalman, Transactions of the ASME–Journal of Basic Engineering **82**, 35 (1960). 10.1115/1.3662552
[25] E. Matthews, et al., Templates of expected measurement uncertainties for fission yields, EPJ Nuclear Sci. Technol. (in review).
[26] A.E. Lovell, et al., EPJ Web Conf. **281**, 00018 (2023). 10.1051/epjconf/202328100018
[27] D.G. Madland, T.R. England, Nuclear Science and Engineering **64**, 859 (1977). 10.13182/NSE77-A14501
[28] C. Sears, et al., Nuclear Data Sheets **173**, 118 (2021), Special Issue on Nuclear Reaction Data. 10.1016/j.nds.2021.04.005
[29] A. Tonchev, private communication (2023)
[30] T. Kawano, et al., Phys. Rev. C **107**, 044608 (2023). 10.1103/PhysRevC.107.044608